Virology 529 (2019) 81–90

Contents lists available at ScienceDirect

Virology

journal homepage: www.elsevier.com/locate/virology

Different forms of African cassava mosaic virus capsid protein within plants and virions

Katharina Hipp[a,*], Kerstin Zikeli[a], Gabi Kepp[a], Lena Schmid[a], Robert L. Shoeman[b], Tomasz P. Jurkowski[c], Tatjana Kleinow[a], Holger Jeske[a]

[a] University of Stuttgart, Institute of Biomaterials and Biomolecular Systems, Department of Molecular Biology and Plant Virology, Pfaffenwaldring 57, 70550 Stuttgart, Germany
[b] Max Planck Institute for Medical Research, Department of Biomolecular Mechanisms, Analytical Protein Biochemistry, Jahnstr. 29, 69120 Heidelberg, Germany
[c] University of Stuttgart, Institute of Biochemistry and Technical Biochemistry, Department of Biochemistry, Allmandring 31, 70550 Stuttgart, Germany

ARTICLE INFO

Keywords:
Geminivirus
Capsid protein
CP
Virus particles
Mass spectrometry
Ubiquitination

ABSTRACT

One geminiviral gene encodes the capsid protein (CP), which can appear as several bands after electrophoresis depending on virus and plant. African cassava mosaic virus-Nigeria CP in *Nicotiana benthamiana,* however, yielded one band (~ 30 kDa) in total protein extracts and purified virions, although its expression in yeast yielded two bands (~ 30, 32 kDa). Mass spectrometry of the complete protein and its tryptic fragments from virions is consistent with a cleaved start M1, acetylated S2, and partial phosphorylation at T12, S25 and S62. Mutants for additional potentially modified sites (N223A; C235A) were fully infectious and formed geminiparticles. Separation in triton acetic acid urea gels confirmed charge changes of the CP between plants and yeast indicating differential phosphorylation. If the CP gene alone was expressed in plants, multiple bands were observed like in yeast. A high turnover rate indicates that post-translational modifications promote CP decay probably via the ubiquitin-triggered proteasomal pathway.

1. Introduction

Since the early days of geminivirology (Esau, 1977; Francki et al., 1979; Goodman et al., 1977; Harrison et al., 1977; Jeske et al., 1977; Matyis et al., 1975), an enigma remains why the unique twin structure of the virions has been developed only in the family of *Geminiviridae* (Jeske, 2009). Whereas icosahedral structures are widespread among viruses (Rossmann, 2013), electron cryo-microscopic studies have revealed that geminiviruses, irrespective of the genera, are composed of two incomplete icosahedra (Böttcher et al., 2004; Hesketh et al., 2018; Hipp et al., 2017; Zhang et al., 2001). In the atomic models, most of the pentameric capsomers fit into a T = 1 symmetry of standard icosahedra, except at the waist, where both capsid halves join with a tilt of 20°. Here, other protein-protein or protein-nucleic acid interactions may be needed for the production of mature geminivirions (Hesketh et al., 2018; Hipp et al., 2017). Two CP bands were found after SDS gel electrophoresis, depending on the virus species and the host (Abouzid and Jeske, 1986; Gorovits et al., 2013a, 2013b) as well as after ectopic expression in fission yeast (referred to as yeast) (Hipp et al., 2016). The different migration behavior may be indicative for post-translational modification of CP, which has been investigated now in plants, in total protein extracts and mature virions.

African cassava mosaic virus (ACMV) belongs to the *Begomovirus* genus of the *Geminiviridae* (Zerbini et al., 2017), with a bipartite genome (DNA A and DNA B) of circular single-stranded (ss) DNA. It is one of the most important pathogens of cassava on the African continent (Legg et al., 2011; Patil and Fauquet, 2009; Rybicki, 2015). The structure of the Kenyan strain (ACMV-[K]) has been determined by electron cryo-microscopy (Böttcher et al., 2004; Hipp et al., 2017). Here, we analyze the closely related ACMV-[N] from Nigeria, because it was reported to be insect-transmissible in contrast to ACMV-[K] (Liu et al., 1999). The geminiviral CPs are multifunctional proteins involved in encapsidation of the genome into virus particles (Böttcher et al., 2004; Hesketh et al., 2018; Hipp et al., 2017; Zhang et al., 2001), insect transmission of the particles (Briddon et al., 1990, 1989; Fischer et al., 2015; Harrison et al., 1977; Höhnle et al., 2001; Kheyr-Pour et al., 2000; Liu et al., 1999; Noris et al., 1998), and transport within the plant (Liu et al., 2001). They interact with each other and host proteins (Hallan and Gafni, 2001; Malik et al., 2005; Yaakov et al., 2011), and bind ss and double-stranded (ds) DNA in a sequence-unspecific manner (Hehnle et al., 2004; Ingham et al., 1995; Liu et al., 1997; Palanichelvam et al., 1998; Priyadarshini and Savithri, 2009).

* Corresponding author. Present address: Max Planck Institute for Developmental Biology, Electron Microscopy, Max-Planck-Ring 5, 72076 Tübingen, Germany.
E-mail address: katharina.hipp@tuebingen.mpg.de (K. Hipp).

https://doi.org/10.1016/j.virol.2019.01.018
Received 27 November 2018; Received in revised form 14 January 2019; Accepted 16 January 2019
Available online 17 January 2019

In the early investigations of geminivirus capsids (Abouzid and Jeske, 1986), two protein bands were observed in denaturing gel electrophoresis analysis. It was uncertain whether one of these bands represents a second protein, encoded by DNA B (BV1) of bipartite begomoviruses, the nuclear shuttle protein (NSP), which has developed probably from gene duplication of AV1 (Kikuno et al., 1984). Both bands, however, were recognized by a single monoclonal antibody raised against purified virus particles (Abouzid, unpublished data) lending further support to the conclusion that they stem from a single gene of DNA A (AV1). In addition, different bands may appear as the result of a plant defence mediated by proteases. Studies on a monopartite begomovirus, tomato yellow leaf curl virus (TYLCV), have investigated this aspect in closer detail (Gorovits et al., 2013a, 2013b). Recently, a double band of the maize streak virus CP has been assigned to a pentameric assembly of the CP in contrast to a single band, the lower one of the double band, found in single, icosahedral capsids and geminate particles (Bennett et al., 2018). It has been speculated that the shift is due to a post-translational modification of the CP (Bennett et al., 2018).

First indications for a post-translational modification were found for Abutilon mosaic virus (AbMV) CP expressed and phosphorylated in *Escherichia coli* (Wege and Jeske, 1998). The precise positions of phosphorylated amino acids in the sequence of the ACMV CP (T12, S25 and S62) were determined by mass spectrometry (MS) (Hipp et al., 2016) after expression of the CP gene in yeast (yCP). The majority of yCP migrated more slowly in SDS gels than ACMV CP from purified particles (pvCP).

Phosphorylation alone may account for the observed differences in migration, but alternative explanations were not excluded. In a number of initial and independent MS experiments, a tryptic peptide of the C-terminus (amino acid 221–249; $CP_{P221–249}$) was missing for pvCP, but not for yCP (Fig. 1c and Suppl. Fig. 1). This peptide attracts special interest, since it is the most conserved sequence among all geminiviral CPs and even for NSP (Kikuno et al., 1984). Thus, a missing portion as a result of processing, either to form the gemini-structure or as a result of proteolytic plant defence, was an alternative option to explain the deviant migration of the lower band. However, improved mass spectroscopic techniques and mutational studies excluded this thesis. The following experiments suggest that differential phosphorylation of CP may be important for some differences in migration behavior. CP phosphorylation may regulate the stability of CP leading to ubiquitination and degradation by the proteasome, if expressed in plants in the absence of replicating geminiviral DNA. This conclusion corresponds to the recent proposal of Hesketh et al. (2018) about the dependence of geminiviral CP stability and replicating ssDNA for assembly of virus particles.

2. Materials and methods

2.1. Construction of plasmids

In order to engineer infectious clones, the mutant plasmids pUC19-APA9-CP^{N223A} and pUC19-APA9-CP^{C235A} were derived from pUC19-APA9 (Kittelmann et al., 2009) by site-directed mutagenesis using primer pairs #1/#2 and #3/#4 (Suppl. Table 1), respectively. After polymerase chain reaction (PCR) (95 °C for 5 min, followed by 20 cycles of 95 °C for 30 s, 49 °C/47 °C for 1 min, and 72 °C for 18 min) with Pfu DNA polymerase (Thermo Fisher Scientific, Darmstadt, Germany), the parental plasmid was digested with DpnI (New England Biolabs (NEB), Frankfurt/Main, Germany), and the PCR products were purified (QIAquick PCR Purification Kit, Qiagen, Hilden, Germany), phosphorylated (T4 polynucleotide kinase, NEB) and ligated (T4 DNA ligase, NEB). The mutant plasmids were transformed into *E. coli* DH5α, amplified and recovered by alkaline lysis. The correctness of the constructs was confirmed by sequencing (Macrogene Europe, Amsterdam, The Netherlands). Compared to the database entry (GenBank accession number AJ427910), pUC19-APA9 showed a nucleotide substitution from CT to AG at position 164/165 (nucleotide numbering according to the AV1 sequence) resulting in an amino acid substitution T55M (Hipp et al., 2016).

To express CP in plants alone, two cloning strategies were followed. First, a BamHI/EcoRI fragment (Fig. 5a) was excised from rolling circle amplification (RCA) amplified ACMV-[N] DNA from plants, named ACMV CP-F. Second, an intron-containing version was established by overlap-PCR (Fig. 5a; Suppl. Table 2), named ACMV CP-I. Both DNAs were inserted into the agrobacterial plasmid pMDC7 by Gateway cloning to permit expression of the respective proteins *in vivo* under the control of an estradiol-inducible promoter as described previously (Curtis and Grossniklaus, 2003; Kleinow et al., 2009). The correctness of the constructs was verified by complete sequencing of the insert.

2.2. Plant infection

Monomer units of wt DNA A of ACMV Nigeria-Ogo (ACMV-[N], GenBank accession number AJ427910) or the corresponding mutated DNAs A (A-CP^{N223A}; A-CP^{C235A}) were released with SphI from plasmids pUC19-APA9, pUC19-APA9-CP^{N223A} or pUC19-APA9-CP^{C235A}. Monomers of wt DNA B (accession number AJ427911) were released with SphI from plasmid pUC19-AP3 (kindly provided by Dr. Rob Briddon, Faisalabad, Pakistan). *N. benthamiana* Domin or *N. occidentalis ssp. hesperis* plants were inoculated with these DNAs mechanically as described (Hipp et al., 2014).

2.3. Protein extraction from plant material

The youngest leaves of ACMV infected or mock inoculated *N. benthamiana* plants were harvested at 7, 14, 21, 28 or 35 days post inoculation (dpi), frozen in liquid nitrogen and stored at − 80 °C until use. Isolation of total proteins was performed according to Von Arnim et al. (1993) with slight modifications: 30 mg of leaves were homogenized with a pestle in liquid nitrogen, and proteins were obtained by addition of 150 µl of extraction buffer (10 mM KCl, 5 mM $MgCl_2$, 400 mM sucrose, 10 mM β-mercaptoethanol, 100 mM TrisHCl pH 8.0, 10% glycerol, 1x Roche Complete EDTA-free protease inhibitor cocktail (Roche, Mannheim, Germany), 1 mM phenylmethylsulfonyl fluoride (PMSF)) and incubation for 30 min at room temperature. Proteins were separated from plant debris by centrifugation for 10 min at 960 × *g*.

Alternatively, leaves were extracted according to Abas and Luschnig (2010) including complex cocktails of proteinase and phosphatase inhibitors, and fractions with enriched larger organelles, microsomes and soluble proteins were collected after centrifugations at 600 × *g*, 2,000 × *g*, and 21,000 × *g*, respectively.

2.4. Virus particle purification

Virus particles were purified by differential and density gradient centrifugation as described (Kittelmann and Jeske, 2008) with the modification of adding protease inhibitors in the homogenization buffer (10 µg/ml protease inhibitor cocktail for plant cell & tissue extracts, Sigma-Aldrich, Taufkirchen, Germany).

2.5. Protein gel electrophoresis and Western blotting

The protein samples were separated in 12.5% SDS-polyacrylamide gels (SDS-PAGE) according to Laemmli (1970) and stained with 0.5% Coomassie brilliant blue (R250, Serva, Heidelberg, Germany, in 50% EtOH, 7% acetic acid) or semi-dry blotted (Bjerrum, 1986) onto nitrocellulose (Protran Nitrocellulose Transfer Membrane, Whatman Schleicher & Schuell, Dassel, Germany) (Method 1). CP was detected using the 1:1000 diluted polyclonal rabbit antiserum AS-0421 (kindly provided by Dr. S. Winter, DSMZ, Braunschweig, Germany), alkaline phosphatase conjugated goat anti-rabbit antibodies (Rockland

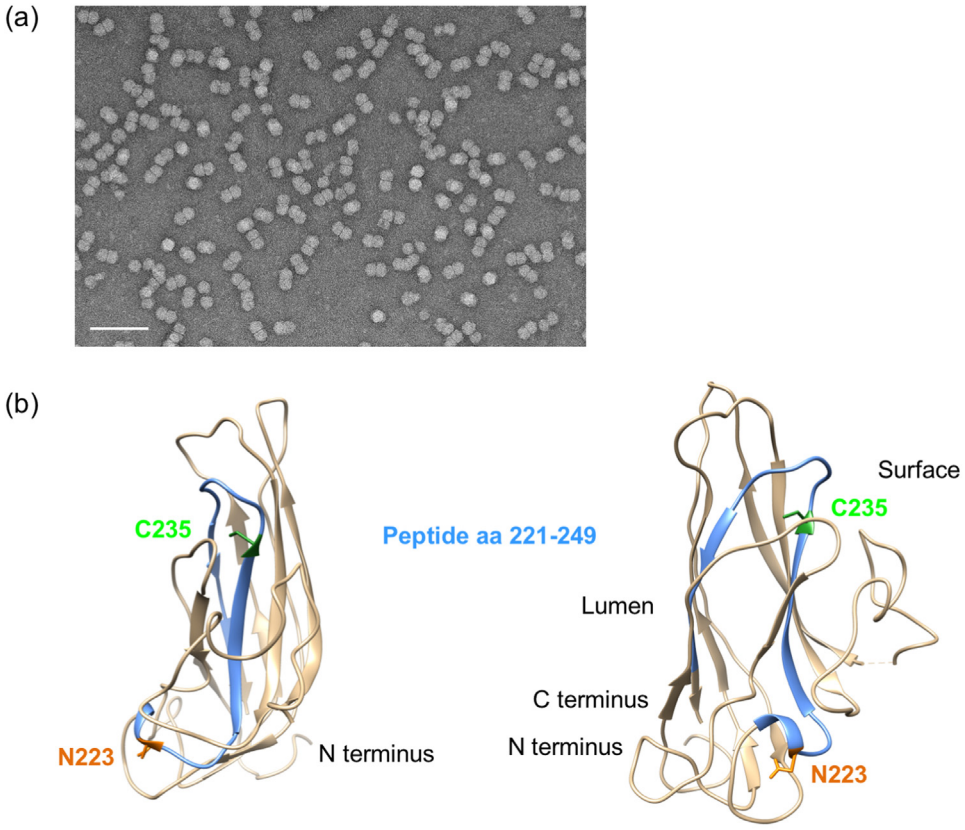

Fig. 1. CP structure and sequence. ACMV particles were purified from infected *N. benthamiana* plants and negatively stained with 2% uranyl acetate for electron microscopy. The particles show the characteristic twinned particle structure, bar: 200 nm. (b) The ACMV CP model (Hipp et al., 2017) is shown in two different orientations. The tryptic peptide (amino acids 221–249) close to the C-terminus that was missing in the initial MS analyses is shown in blue including N223 (orange) and C235 (green). (c) The amino acid sequence of the ACMV CP is shown in one letter code highlighting M55 (yellow background, variation from the database entry), the C-terminal "missing" peptide (blue background) and cleavage sites for trypsin indicated by red lines. Several possible modification sites within the blue-highlighted peptide are shown: blue arrows – predicted phosphorylation sites Y221 and Y243 (NetPhos2.0 Server), orange arrow – potential N-glycosylation site N223, green arrow – potential S-acylation site C235, red arrow – predicted O-linked β-*N*-acetylglucosamine S239 (YingOYang 1.2 Server). The black line marks the peptide (aa 221–233) used for generating the peptide antibody.

Immunochemicals, Inc., Gilbertsville, PA, USA), and nitro-blue tetrazolium choride, 5-bromo-4-chloro-3′-indolylphosphate (NBT/BCIP).

Alternatively, the CP was detected using the 1:2500 diluted polyclonal antiserum α-ACMV-KNCP #2 raised against the peptide YENHTENALLLYM (CP amino acid sequence 221–233) in rabbits (pab productions, Hebertshausen, Germany), and secondary antibodies and substrate as described before.

For more sensitive detection (Method 2), the SDS gel was equilibrated for 15 min in transfer buffer (50 mM Tris, 50 mM boric acid, 10% methanol) before semi-dry blotting onto methanol-activated PVDF membrane was done at 20 V for 30 min. The membrane was rinsed with TBS-T (20 mM Tris-HCl pH7.6; 138 mM NaCl plus 0.1% Tween-20) for 5 min, blocked for 1 h in 5% BSA, Normal Goat Serum (Jackson ImmunoResearch Europe Ltd, Ely, UK, 1:10,000), TBS-T at room temperature and incubated overnight at 4 °C with antiserum AS-0895 (kindly provided by Dr. S. Winter; diluted 1:10,000 in blocking solution), which had been purified by cross-absorption to plant proteins from *N. benthamiana* plants agroinfiltrated with P19-expression plasmids. After several washing steps (1x short, 1 × 15 min, 4 × 5 min in TBS-T), the secondary antibody (goat anti-rabbit horse radish peroxidase, 1:10,000 in blocking solution; Biotrend, Köln, Germany) was added for 1 h at room temperature, followed by washing steps (1x short, 1 × 15 min, 3 × 5 min in TBS-T and 1 × 15 min in TBS). Signal detection was performed using the substrate of the Luminata Crescendo Western HRP kit (Merck Millipore, Darmstadt, Germany) and exposure to X-ray film. For stripping, the membrane was incubated in 62.5 mM Tris-HCl pH 6.8 plus 2% SDS at 60 °C for 20 min and washed in TBS-T for 2 × 5 min at room temperature. After blocking as before, a mouse monoclonal antibody against ubiquitinated proteins (Biotrend, Köln, Germany; clone FK2; 1:20,000 in blocking solution) was applied at 4 °C overnight and developed as described.

Triton/acetic acid/urea (TAU) polyacrylamide gels were prepared as described (Ryan and Annunziato, 2001; Shechter et al., 2007) with some modifications: The samples were incubated with sulfuric acid (final concentration: 0.2 M) overnight at 4 °C and centrifuged for 10 min at 12,000 × *g* and 4 °C. Acid extracted proteins were transferred from the supernatant into a fresh tube and precipitated by adding trichloroacetic acid (TCA, final concentration: 33%) and incubation for 30 min at 4 °C. Precipitated proteins were recovered by centrifugation for 10 min at 12,000 × *g* and 4 °C and washed twice with ice-cold acetone. The final pellet was air-dried and resuspended in TAU sample buffer (5.8 M urea, 5% acetic acid, 16% glycerol, 0.2% methyl green, 4.8% β-mercaptoethanol). Proteins from 100 µl fractions of density gradient purified virus particles were precipitated with TCA prior to sulfuric acid treatment.

TAU gels were pre-run in running buffer (5% acetic acid) for 3.5 h at

350 V and in scavenger solution (2.12 M β-mercaptoethylamine, 2.5 M urea, 4.8% acetic acid) for 3 h at 300 V. After loading the samples, the electrophoresis was done for 15 min at 400 V followed by 16.5 h at 200 V. The gels were then incubated with 20% TCA for 30 min and twice with 50% ethanol for 30 min, and either stained with Serva Violet 17 (SERVA Electrophoresis GmbH, Heidelberg, Germany) or Western blotted (Method 3) onto nitrocellulose described above for 30 min at 20 V after pre-equilibration for 15 min in transfer buffer (50 mM Tris, 50 mM boric acid, 10% methanol) containing 1% SDS and 10 min in transfer buffer without SDS. Membranes were developed as described for Method 1.

2.6. Mass spectrometry

Initial MS experiments on the CP proteins were performed via matrix-assisted laser desorption/ionization-time-of-flight (MALDI-TOF) MS, essentially as previously described for peptide map fingerprinting experiments (Wulfmeyer et al., 2012) and for intact mass experiments (Khoo et al., 2007).

Wt and mutant CP from purified virus particles were separated by SDS-PAGE to excise the CP bands after Coomassie staining. For the improved MS experiments, in gel trypsin-digestion and NanoLC-ESI-MS/MS was performed by the Core Facility Hohenheim Module Mass Spectrometry, University of Hohenheim, Stuttgart, Germany.

2.7. Extraction of nucleic acids/RCA-RFLP

Total nucleic acids from plants infected with wt or mutant viral DNA were prepared at 10 dpi, and viral DNAs were amplified by RCA and analyzed for restriction fragment length polymorphism (RFLP) with HpaII on 1.5% agarose gels as described in Hipp et al. (2014).

2.8. Transmission electron microscopy

Samples of purified wt or mutant virus particles were negatively stained with 2% uranyl acetate on glow-discharged Formvar- and carbon-coated copper grids. Samples were analyzed with an FEI Tecnai G^2 operated at 200 kV (FEI, Eindhoven, The Netherlands), and images were recorded with a Tietz TemCam-F416 CMOS camera (TVIPS, Gauting, Germany).

3. Results

The virus investigated in this study is based on a bacterial clone of an ACMV strain (ACMV-[N]). It differs from ACMV-[K] in several amino acid positions which might be relevant for particle formation and whitefly transmission (Liu et al., 1999). The sequence of the clone propagated in our laboratory compared to the data base sequence of ACMV-[N], revealed one further amino acid exchange T55M, which is frequently found among isolates of ACMV from African fields and may be part of a natural polymorphism and not a defect. The structure of ACMV-[N] as revealed by negative staining was indistinguishable from ACMV-[K] (Fig. 1a). Therefore, it is appropriate to use the CP model derived for ACMV-[K] (Fig. 1b) to map potential effects of modifications and processing steps (Fig. 1c) on the structure.

3.1. Only a single CP band was detected in total proteins from plants

Starting from the observation that the ACMV CP occurred in two electrophoretic forms when expressed in fission yeast, but only in a single form if the CP was derived from purified particles isolated from infected plants, we investigated the fate of the CP within plants.

During the course of an infection of *N. benthamiana* plants, only one CP band was detectable in total protein extracts (Fig. 2a). The electrophoretic mobility of this pCP was similar to that from virions (pvCP; Fig. 2b, Suppl. Fig. 2) as well as to the minor and lower band of yCP (Fig. 2b, Suppl. Fig. 2, and Hipp et al., 2016). The calculated apparent molecular masses were determined as 29–30 kDa for pCP and the lower yCP band, whereas 31–32 kDa were determined for the upper yCP band in different gels (Fig. 2b, Suppl. Fig. 2). The lower band was in the range of the expected value calculated from the translated sequence (30.2 kDa for the complete sequence, 30.1 kDa if the initiator M is removed and the resulting N-terminal S is acetylated).

To determine the mass of the CP independent of SDS-PAGE, undigested pvCP was analyzed by MS revealing a single peak at 30.109 kDa (Fig. 2c), approximating the expected CP mass without initiator M1 and with acS2 within the limits of determination (20 Da larger, or 4 Da larger if an internal M was oxidized).

For trypsin-digested proteins, an initial series of five independent MALDI-TOF experiments (Suppl. Fig. 1) revealed a major difference between yCP and pvCP: the fragment comprising amino acids 221–249 was not detectable in diverse plant samples (Fig. 1b, c, peptide highlighted blue). This peptide is close to the C-terminus of the protein and part of the jelly roll motif in the CP model (Fig. 1b, and Hipp et al., 2017). As expected from the structure, it is highly conserved among begomoviral sequences.

In order to investigate the presence of this peptide in the CP, an antibody was raised against the CP peptide 221–233 (Fig. 1c) and used in Western blot detection (Suppl. Fig. 2). The pCP in total proteins as well as the yCP were detected specifically by the peptide antibody suggesting that the failure to detect the peptide via MALDI-TOF MS may be a technical problem rather than an indication of protein processing.

3.2. CP mutants in the C-terminal peptide

In order to investigate if post-translational modifications prevented the detection of the C-terminal peptide, two CP alanine mutants (mut CPs) were generated to impair either a potential glycosylation of N223 or acylation of C235 (Fig. 1c), modification sites that have been predicted bioinformatically. The respective progeny viruses were infectious in *N. benthamiana* and *N. occidentalis* with an infection rate comparable to the wt virus (Table 1), and plants showed the typical ACMV symptoms (Suppl. Fig. 3a). Infected plants accumulated viral DNA (Suppl. Fig. 3b), and retained the respective mutations in the CP (data not shown). Both mutants were proficient in virus particle assembly and showed the characteristic geminivirus particle structure in electron microscopy after virus particle purification from infected plants (Suppl. Fig. 4a-f). The wt and mut CPs from purified virus particles that migrated with similar mobility and as a single band in SDS-PAGE and on Western blots (Suppl. Fig. 4g, data not shown), were further analyzed by mass spectrometry (nanoLC-ESI-MS/MS, Fig. 3). All three CPs were processed at the N-terminus: the initiator M was cleaved and S2 acetylated. Furthermore, wt CP as well as both mutants were found to be phosphorylated partially at T12, S25 and S62 (Fig. 3; highlighted green), the same positions identified as phosphorylated for the yCP (Hipp et al., 2016). Interestingly, the missing peptide was detected in all three CP variants (Fig. 3), and no post-translational modifications were detectable in this area.

3.3. Differential mobility of plant- and yeast-derived CP during charge-dependent gel electrophoresis

After having excluded that the differences in electrophoretic mobility in SDS-PAGE are caused by proteolytic cleavage of CP as highly unlikely (Fig. 2b, Suppl. Fig. 2, Fig. 3) and post-translational modifications in the C-terminal peptide do not seem to play a role, the alternative option of charge differences was examined. TAU-PAGE, a system that has been used to separate differentially post-translationally modified histone species (Ryan and Annunziato, 2001; Shechter et al., 2007) was employed. The technique has the potential to resolve isoforms that differ in one phosphate group. Proteins from yeast (yCP) as well as from plants, CP either from purified virus particles (pvCP) or

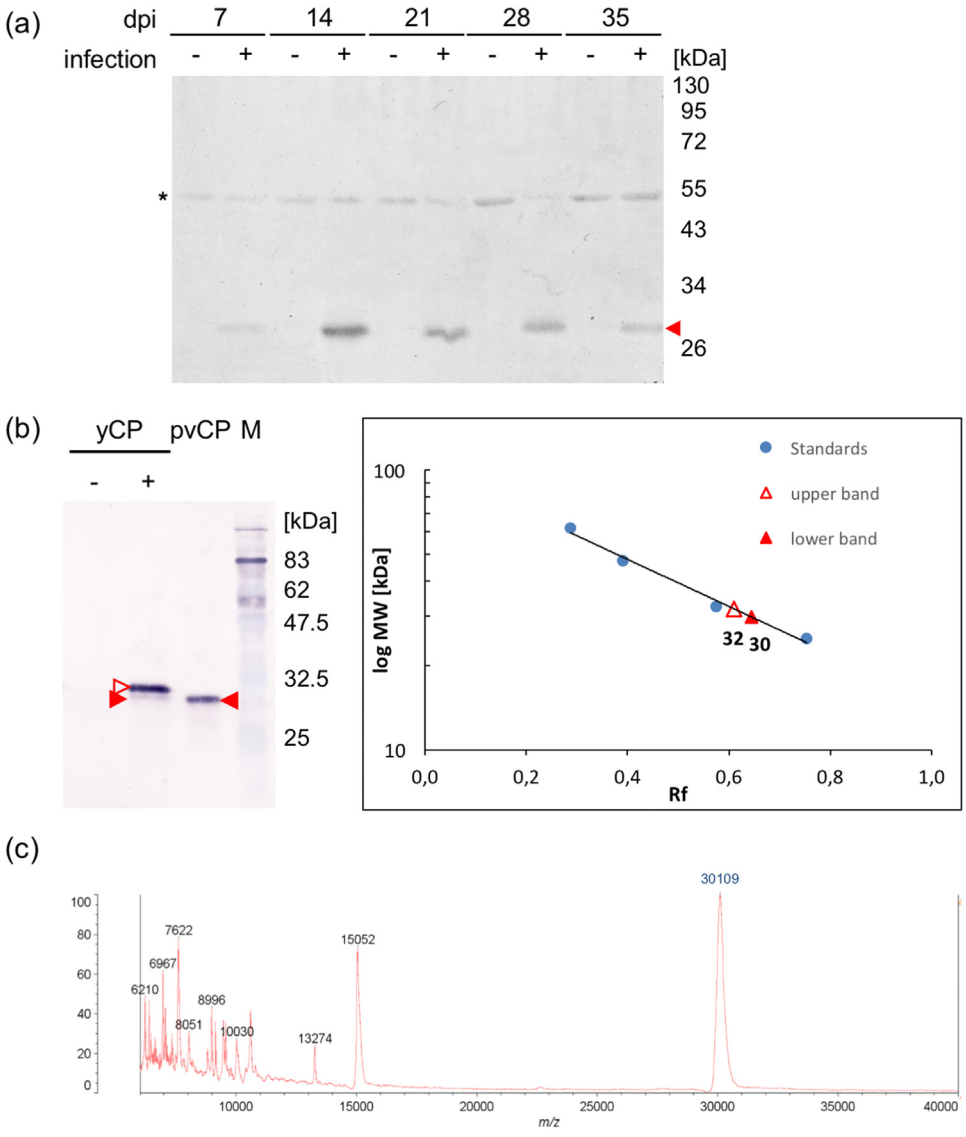

Fig. 2. Time course of pCP. Leaves from *N. benthamiana* plants infected with ACMV (+) or mock-inoculated (-) were harvested at 7, 14, 21, 28 or 35 days post infection (dpi). Total proteins were isolated and separated by SDS-PAGE. pCP was detected after Western blotting with 1:1000 diluted AS-0421. The position of the pCP is marked by a red arrowhead; the asterisk indicates the position of a cross-reacting plant protein. The positions of the marker proteins (M) with their molecular masses are shown on the right. (b) Comparison of pvCP and yCP. The CP expressed in yeast (yCP, +, -: repressed, samples harvested 18 h post induction (hpi)) was compared to plant-derived CP from partially purified virus particles (pvCP). yCP can be separated into an upper (open arrowhead) and a lower band (filled arrowhead) that has the same mobility as pvCP (filled arrowhead). The apparent molecular masses of the CP in the upper (ca. 32 kDa) and lower bands (ca. 30 kDa) were calculated with reference to the marker proteins (diagram). (c) Purified virus particles from infected plants were analyzed by MS after dialysis against 0.1 M sodium borate buffer pH 8.0. The *m/z* of the largest peak is 30,109 Da, which is approximately the mass expected for the CP minus initiator M with S2 acetylated and an internal M oxidation (30,104 Da). The 15,052 Da peak corresponds to the + 2 state of the CP. *m/z*: mass divided by charge number.

Table 1
Infection rate of plants inoculated with wt or mut CP virus.

Inoculum[a]	*N. benthamiana*					*N. occidentalis ssp. hesperis*	
	Exp. #1	Exp. #2	Exp. #3	Exp. #4	I.r.[c]	Exp. #1	I.r.[c]
A + B	16/29[b]	13/29	10/29	10/10	51	6/6	100
A-CP^{N223A} + B	24/29	14/29	15/29	10/10	65	7/7	100
A-CP^{C235A} + B	23/29	9/29	9/29	10/10	53	7/7	100
Mock	0/5	0/5	0/5	0/12	0		
B	0/10			0/3	0	0/3	0

[a] A: monomer of wt ACMV DNA A; A-CP^{N223A}: monomer of ACMV DNA A with the CP N223A mutation; A-CP^{C235A}: monomer of ACMV DNA A with the CP C235A mutation; B: monomer of wt ACMV DNA B; mock: water.

[b] Number of plants showing symptoms/total number of plants inoculated with the indicated combination.

[c] I.r.: overall infection rate, numbers given in %.

directly from total protein extracts (pCP) of infected plants were acid-extracted and separated by TAU-PAGE (Fig. 4). Whereas both the pCP and pvCP showed a similar mobility (Fig. 4, filled triangles), the majority of yCP showed a lower mobility (Fig. 4, open triangles) and only a very faint signal was observed with the same mobility behavior as pvCP (Fig. 4, filled triangle). This finding is consistent with a differential phosphorylation of yCP and pCP.

3.4. The fate of CP in plants when expressed without replicating ssDNA

In order to examine whether the observed shift of CP bands in SDS-PAGE is a specific feature of yeast expression or relevant for plants, several plasmids were constructed to express ACMV-[N] CP under the control of plant promoters. The best results we could obtain in many independent experiments are documented in Suppl. Fig. 5, with 2x cauliflower mosaic virus 35S promoter and tobacco mosaic virus omega translational enhancer (Kadri et al., 2011) and with or without inserted intron. They show that even under optimal conditions for the parallel expression of GFP, CP signals are visible only at the limit of detection. At the same time, these experiments excluded a harmful effect of CP to plant cells, since no difference was observed for GFP in the presence or absence of CP. An alternative explanation is a short life time of the CP if expressed out of the context of a viral infection.

To test this hypothesis, ACMV-[N] CP constructs were established that express the target protein under the control of an estradiol-inducible promoter (Curtis and Grossniklaus, 2003; Kleinow et al., 2009), in order to follow the fate of CP after induction. This approach improved the detection considerably, although at a still low signal

```
CP wt    MSKRPGDIII STPGSKVRRR LNFDSPYRNR ATAPTVHVTN RKRAWINRPM -50
CP N223A MSKRPGDIII STPGSKVRRR LNFDSPYRNR ATAPTVHVTN RKRAWINRPM
CP C235A MSKRPGDIII STPGSKVRRR LNFDSPYRNR ATAPTVHVTN RKRAWINRPM

CP wt    YRKPMMYRMY RSPDIPRGCE GPCKVQSYEQ RDDVKHLGIC KVISDVTRGP -100
CP N223A YRKPMMYRMY RSPDIPRGCE GPCKVQSYEQ RDDVKHLGIC KVISDVTRGP
CP C235A YRKPMMYRMY RSPDIPRGCE GPCKVQSYEQ RDDVKHLGIC KVISDVTRGP

CP wt    GLTHRVGKRF CIKSIYILGK IWMDENIKKQ NHTNNVMFYL LRDRRPYGNA -150
CP N223A GLTHRVGKRF CIKSIYILGK IWMDENIKKQ NHTNNVMFYL LRDRRPYGNA
CP C235A GLTHRVGKRF CIKSIYILGK IWMDENIKKQ NHTNNVMFYL LRDRRPYGNA

CP wt    PQDFGQIFNM FDNEPSTATI KNDLRDRFQV LRKFHATVIG GPSGMKEQAL -200
CP N223A PQDFGQIFNM FDNEPSTATI KNDLRDRFQV LRKFHATVIG GPSGMKEQAL
CP C235A PQDFGQIFNM FDNEPSTATI KNDLRDRFQV LRKFHATVIG GPSGMKEQAL

CP wt    VKRFYRLNHH VTYNHQEAGK YENHTENALL LYMACTHASN PVYATLKIRI -250
CP N223A VKRFYRLNHH VTYNHQEAGK YEAHTENALL LYMACTHASN PVYATLKIRI
CP C235A VKRFYRLNHH VTYNHQEAGK YENHTENALL LYMAATHASN PVYATLKIRI

CP wt    YFYDSIGN
CP N223A YFYDSIGN
CP C235A YFYDSIGN
```

Fig. 3. Mass spectrometry of wt and mut CP from purified virus particles. The amino acid sequence of the wt CP, CP^{N223A} and CP^{C235A} are shown with amino acids on yellow background if unmodified, on green background for modification by phosphorylation (T12, S25, S62), and on an orange background for acetylation of S2. Peptides with a white background have not been identified. Amino acids changed in CP^{N223A} and CP^{C235A} are highlighted in red font.

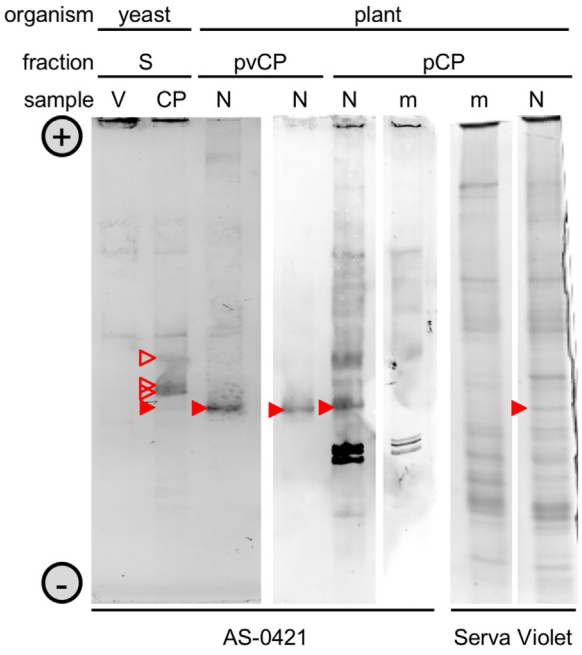

Fig. 4. Electrophoretic mobility of ACMV CP in TAU gels. Cell extract supernatants (fraction S) were prepared from yeast cells expressing the CP or vector control cells (V) harvested at 9 hpi. Virus particles (pvCP) were purified from ACMV-[N]-infected (N) *N. benthamiana* plants by density gradient centrifugation. Samples from *N. benthamiana* plants (pCP) infected with ACMV-[N] (N) or mock-inoculated (M) were homogenized, and together with the other samples prepared for TAU gel electrophoresis by sulfuric acid treatment. Gels were either stained with Serva Violet or blotted onto nitrocellulose membranes followed by immunodetection of the CP. The different forms of the CP are indicated by open and filled arrowheads. Electric poles of the gel are marked by (+) and (-).

intensity (Fig. 5). A similar band pattern like for yCP was visible in addition to a novel band (apparent molecular mass 38 kDa) that may be informative and may explain the fate of the CPs as the calculated difference to unmodified CP is ~8 kDa close to the molecular mass of ubiquitin (8.5 kDa). Correspondingly, signals in ladder and increasing signals at the position of high molecular weight proteins (Fig. 5b; hmw) are consistent with an interpretation of a specific removal of CP by the ubiquitin proteasome degradation pathway. There is an increase of the 38 kDa band as well as the high molecular weight proteins over time of CP expression whereas the amount of unmodified CP seems to decrease after 24 h post estradiol induction (hpei) compared to the 12 hpei time point (Fig. 5). The multitude of bands and the ladder under best resolution is shown in Fig. 6. The evaluation of the migration behavior revealed a neat stepwise increase of 8.5 kDa for the apparent molecular masses of the ladder, most prominent for the CP-I construct at 12 hpei in the 2000 × *g* pellet. Most CP with a molecular mass between 30 and 32 kDa was found in the fraction of enriched nuclei (Fig. 6; 2000 × *g*), whereas the relative abundance of the 38 kDa protein is higher in the fraction of soluble proteins and may result from disrupted organelles and/or the cytoplasmic pool. Incubation of the same blot, after stripping, with a monoclonal antibody raised against ubiquitinated proteins (Fig. 6; U) confirmed that the 38 kDa band represents ubiquitinated CP (Fig. 6; CP: Ub) for the 21,000 × *g* pellet of CP-F as well as CP-I. The most parsimonious current explanation of these results is that out of context CP is phosphorylated, triggering ubiquitination and degradation to yield the low steady state levels of CP found here (Figs. 5 and 6) and in previous experiments (Suppl. Fig. 5).

4. Discussion

The ACMV-[N] CP derived from virus-infected *N. benthamiana* plants was analyzed by MS, mutational experiments and gel electrophoresis to gain insights into potential processing events that may regulate the assembly of the characteristic geminivirus particles. In order to form the intriguing twinned particles from a single CP, one might envisage a processing of some of the proteins, either those that establish the contact between the two halves of the particle and form the waist, or the others that are found in an icosahedral environment (Böttcher et al., 2004; Hesketh et al., 2018; Hipp et al., 2017; Kittelmann and Jeske, 2008). However, alternative explanations are possible: (1) The CP might be flexible enough to accommodate all the different positions in the virus particle as described recently for Ageratum yellow vein virus (AYVV) and the Kenyan strain of ACMV (Hesketh et al., 2018; Hipp et al., 2017). (2) Post-translational modifications may be important during maturation of virus particles, as it has been observed for other viruses like bacteriophage HK97 from prohead I to prohead II (Gertsman et al., 2009; Huang et al., 2011) or herpesviruses (Mou et al., 2009; Schmidt et al., 2010; Wisner et al., 2009). Interestingly, phosphorylation of the geminiviral tomato golden mosaic virus replication initiator protein impaired binding of the protein to DNA (Shen et al., 2018). (3) The half-life of the protein may be controlled by a selective decay, where phosphorylation precedes ubiqutination and proteasomal degradation, as described for an RNA plant

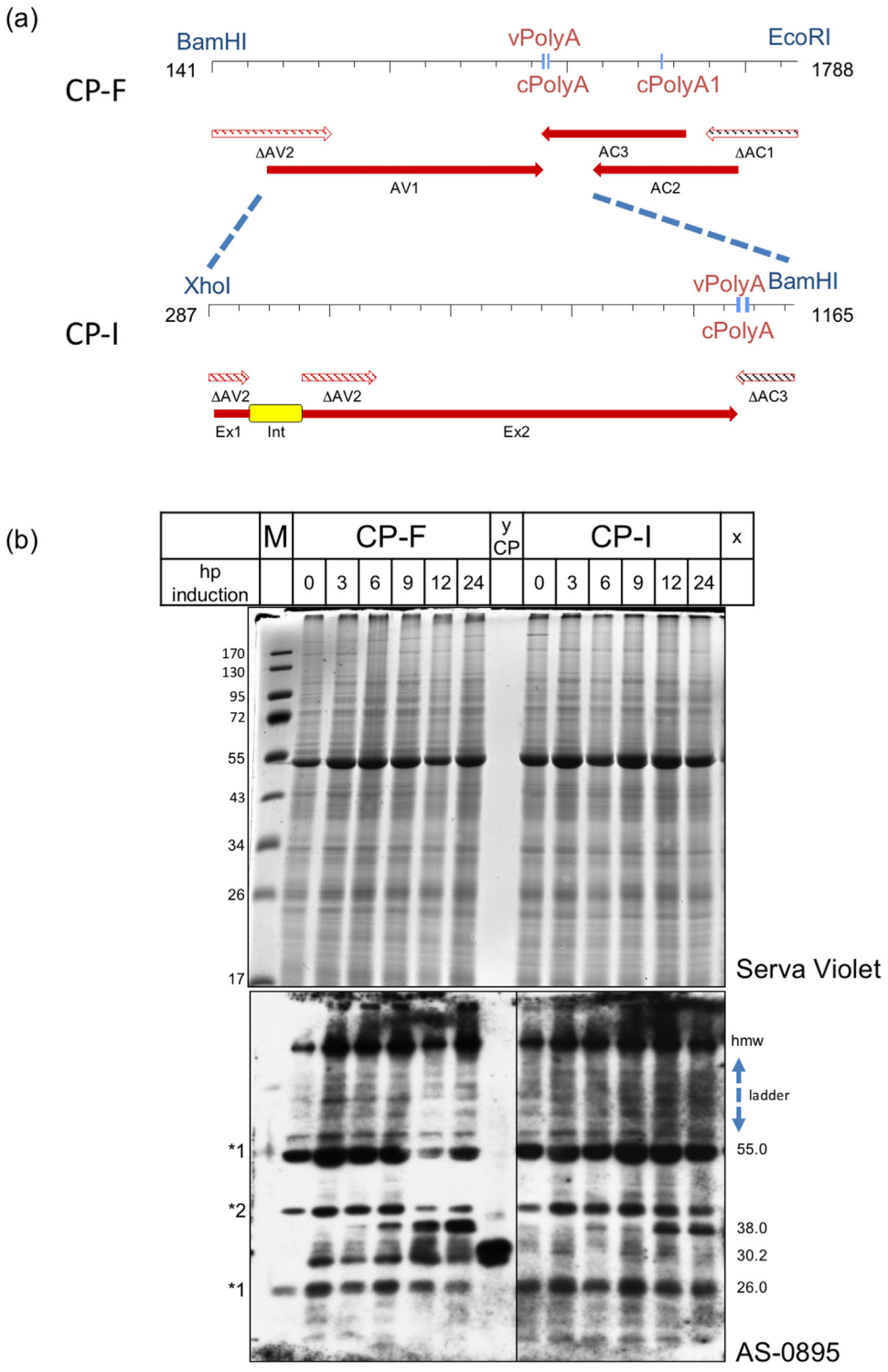

Fig. 5. Expression of ACMV-[N] CP alone in plants using Western blot method 2. (a) Two expression cassettes were constructed based on the BamHI-EcoRI fragment of ACMV-[N] DNA A (CP-F) or on overlap PCR (see Suppl. Table 2; CP-I). ACMV terminator elements for viral (v) and complementary (c) strand (PolyA), truncated ORFs (Δ), exons (Ex), intron (Int) and genomic positions (left, right) of the fragments are indicated. (b) After inserting the expression cassettes into plasmid vectors for estradiol inducible expression and transformation of agrobacteria, leaves were agroinoculated and 19 h later induced by estradiol. The time course between 0 and 24 h post estradiol induction (hpei) is shown for CP-F and CP-I in comparison with yeast-expressed CP (yCP). Low-speed pellets (600 × *g*, 2000 × *g*) according to Abas and Luschnig (2010) were separated and stained with Serva Violet (upper part). Western blot was developed with polyclonal anti-ACMV antiserum (AS-0895, lower part; exposure times 5 for left or 15 min for right blot). The apparent molecular masses for the bands are indicated on the right, with the predicted molecular mass of ACMV-[N] CP without modifications of 30.2 kDa. hmw: signals for high molecular weight proteins. * 1: cross-reacting host proteins; * 2 cross-reacting proteins upon agroinoculation.

virus (turnip yellow mosaic virus) (Héricourt et al., 2000; Jupin et al., 2017). This pathway is regulated by a complex network of ubiquitinating and de-ubiquitinating enzymes in plants (Ewan et al., 2011; Genschik et al., 1998; Lozano-Duran and Bejarano, 2011; McDowell and Philpott, 2013; Romero-Barrios and Vert, 2018; Sahtoe and Sixma, 2015; Sato et al., 2014; Stes et al., 2014; Walton et al., 2016).

For ACMV-[N] CP during infection, our analyses revealed no hint for a time-dependent processing, and the mature virion harbored a predominant protein with the molecular weight of the predicted primary sequence with cleaved initiator M1 and acetylated S2 (Fig. 2). Nevertheless, small portions of tryptic fragments were resolved that were phosphorylated, when extracted from gel-purified pvCP (Fig. 3). The sites of potential phosphorylation (T12, S25, S62) are located within the N-terminal region of the CP, which is important for DNA binding and nuclear localization (Unseld et al., 2004, 2001, and references therein). In the atomic models built based on the cryo-EM maps, the N-terminus of the CP was resolved starting with amino acid 63 for most subunits and extended up to amino acid 40 for subunits in the waist (Hesketh et al., 2018; Hipp et al., 2017). Correspondingly, a potential differential phosphorylation within the capsid of amino acids

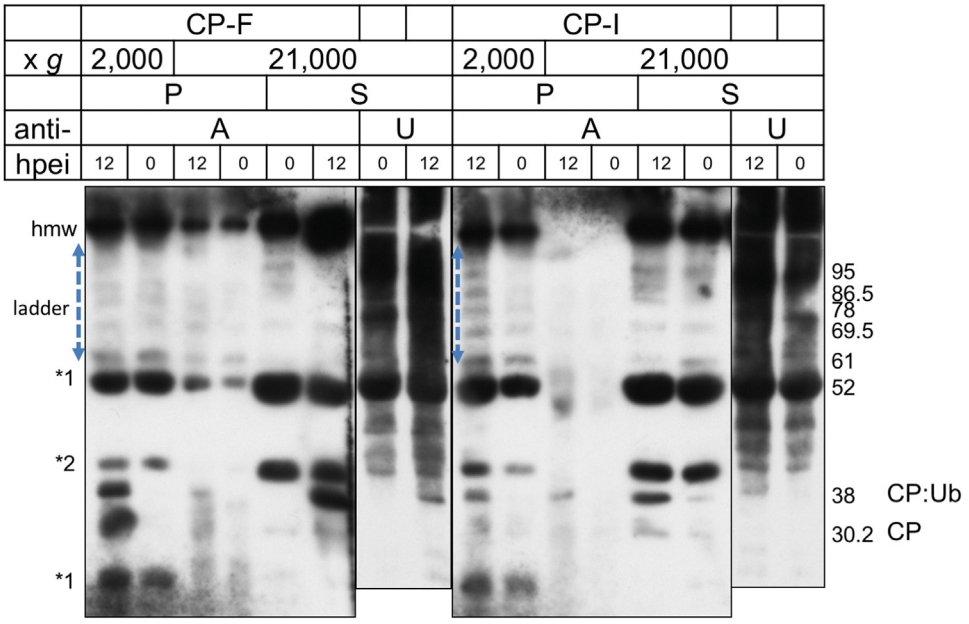

Fig. 6. Expression of ACMV-[N] CP as described in Fig. 5 at 0 and 12 hpei for different enrichment fractions: for larger organelles (2000 × *g* pellet, P), microsomes (21,000 × *g* P) and soluble proteins (21,000 × *g* supernatant, S). Note the ladder between 61 and 95 kDa, which fits to steps of 8.5 kDa, the molecular mass of ubiquitin. The Western blot was first incubated with anti-ACMV antiserum AS-0895 (A), and, after stripping, with a monoclonal antibody against ubiquitinated proteins (U).

determined by mass spectrometry was not visible in the reconstructions. Our initial mass spectrometry of CP derived from purified virus particles has missed a tryptic peptide within the C-terminus and previous Western blot analyses gave hints for a further proteolytic processing (Unseld et al., 2004). The sequence of the missing peptide is highly conserved among begomoviruses and comprises part of the core β-barrel structure in the CP model. Since the CP expressed in fission yeast showed the missing peptide (Hipp et al., 2016), it was mandatory to scrutinize whether this observation was due to the purification protocol rather than a processing in plants. In order to exclude an internal processing event in the plants that could result from an excision of a stretch of subsequent amino acids (Eryilmaz et al., 2014; Novikova et al., 2014), CP samples were probed with a peptide antibody generated against a part of the missing fragment. The antibody recognized both the yeast- and plant-derived CP making an internal processing in this part of the protein unlikely. In addition, we tried to assess specific positions in this region by mutagenesis. Two modifications that might impede detection by mass spectrometry are glycosylation of N223 and acylation of C235. Both alanine mutants behaved like the wt in the context of a viral infection in *N. benthamiana* plants with respect to symptoms, accumulation of viral DNA, and assembly of the characteristic twinned virus particles. An improved mass spectrometry employing LC separation of the viral peptides and nanoESI ionization of the wt CP and both mutants revealed the missing peptide for the first time, and no modifications were detected therein. However, the CP variants were processed at the N-terminus with the initiator M cleaved, as it has been shown for yCP (Hipp et al., 2016), and the same phosphorylation sites were identified within the N-terminus: T12, S25 and S62. These residues are quite conserved among geminivirus sequences at the exact or close-by position sometimes interchanged with a serine or threonine, respectively. Compared to the pCP variants, the yCP showed no acetylation of S2 (Hipp et al., 2016).

The difference in electrophoretic mobility in SDS-PAGE between pCP and yCP in the upper band is probably due to a differential phosphorylation based on the analysis in charge-dependent TAU gels (Fig. 4), where most of the yCP was migrating considerably more slowly as it has been shown for differentially modified histones in this gel system (Ryan and Annunziato, 2001; Shechter et al., 2007).

In contrast to a single band in SDS-PAGE during a viral infection or from purified virus particles, several bands with similar migration as yCP were detected after CP expression *in planta* without the viral infection. Moreover, ubiquitinated forms were identified by size-determination and specific antibodies (Figs. 5 and 6) indicating that free ACMV-[N] CP is readily targeted for degradation by the ubiquitin-proteasomal pathway. These results explain the low steady state level of the protein during ectopic expression in plants in contrast to yeast and to viral infection. An involvement of a ubiquitin-dependent degradation by the proteasome has been discussed for the CP of TYLCV recently (Gorovits et al., 2016, 2014).

The lack of acetylated S2 and the differential phosphorylation of yCP may explain why this protein was able to condense and complex ssDNA, but failed to assemble true gemini-like particles (Hipp et al., 2016).

In summary, we conclude that one CP form is sufficient to assemble into the geminate virus particles in the presence of viral DNA in plants in accordance with a recently proposed model of geminate particle formation (Hesketh et al., 2018). Improved purification and analytical protocols excluded a substantial modification of the CP in mature virions. Using estradiol-inducible constructs and enrichment protocols with cocktails of proteinase and phosphatase inhibitors, however, enabled the demonstration that complex modifications take place in plants as well, although at a low level of detection. Whether phosphorylation plays a role in early maturation, regulation of nuclear import and/or specific decay cannot be decided at this moment and needs further investigation.

Acknowledgments

We thank Dr. Rob Briddon for providing cloned ACMV-[N]-DNA, Dr. Nam-Hai Chua (Rockefeller University, New York, USA) for providing plasmid pMDC7, Dr. Stephan Winter for providing antisera and the gardeners, Annika Allinger, Diether Gotthardt and Marvin Müller, for taking care of the plants. We are grateful to Dr. Jens Pfannstiel and colleagues at the Core Facility Hohenheim Module Mass Spectrometry, University of Hohenheim, Stuttgart, Germany, for performing the mass spectrometry. We also thank Prof. Dr. Bettina Böttcher and Prof. Dr. Christina Wege for critically reading the manuscript.

Compliance with ethical standards

Funding

This study was funded by DFG (Je 116/11-1) and Senator-Eiselen-Vermächtnis.

Conflict of interest

The authors declare that they have no conflict of interest.

Ethical approval

This article does not contain any studies with human participants or animals performed by any of the authors.

Appendix A. Supplementary material

Supplementary data associated with this article can be found in the online version at doi:10.1016/j.virol.2019.01.018

References

Abas, L., Luschnig, C., 2010. Maximum yields of microsomal-type membranes from small amounts of plant material without requiring ultracentrifugation. Anal. Biochem. 401, 217–227. https://doi.org/10.1016/j.ab.2010.02.030.

Abouzid, A., Jeske, H., 1986. The purification and characterization of gemini particles from Abutilon mosaic virus infected Malvaceae. J. Phytopathol. 115, 344–353.

Bennett, A., Rodriguez, D., Lister, S., Boulton, M., McKenna, R., Agbandje-McKenna, M., 2018. Assembly and disassembly intermediates of maize streak geminivirus. Virology 525, 224–236. https://doi.org/10.1016/j.virol.2018.09.011.

Bjerrum, O.J., 1986. Buffer systems and transfer parameters for semidry electroblotting with a horizontal apparatus. In: Dunn, M.J. (Ed.), Proceedings of the Fifth Meeting of the International Electrophoresis Society. VHC, Weinheim, Germany, pp. 315–327.

Böttcher, B., Unseld, S., Ceulemans, H., Russell, R.B., Jeske, H., 2004. Geminate structures of African cassava mosaic virus. J. Virol. 78, 6709–6714.

Briddon, R.W., Pinner, M.S., Stanley, J., Markham, P.G., 1990. Geminivirus coat protein gene replacement alters insect specificity. Virology 177, 85–94.

Briddon, R.W., Watts, J., Markham, P.G., Stanley, J., 1989. The coat protein of beet curly top virus is essential for infectivity. Virology 172, 628–633.

Curtis, M.D., Grossniklaus, U., 2003. A gateway cloning vector set for high-throughput functional analysis of genes in planta. Plant Physiol. 133, 462–469. https://doi.org/10.1104/pp.103.027979.

Eryilmaz, E., Shah, N.H., Muir, T.W., Cowburn, D., 2014. Structural and dynamical features of inteins and implications on protein splicing. J. Biol. Chem. 289, 14506–14511. https://doi.org/10.1074/jbc.R113.540302.

Esau, K., 1977. Virus-like particles in nuclei of phloem cells in spinach leaves infected with curly top virus. J. Ultrastruct. Res. 61, 78–88.

Ewan, R., Pangestuti, R., Thornber, S., Craig, A., Carr, C., O'Donnell, L., Zhang, C., Sadanandom, A., 2011. Deubiquitinating enzymes AtUBP12 and AtUBP13 and their tobacco homologue NtUBP12 are negative regulators of plant immunity. New Phytol. 191, 92–106. https://doi.org/10.1111/j.1469-8137.2011.03672.x.

Fischer, A., Strohmeier, S., Krenz, B., Jeske, H., 2015. Evolutionary liberties of the Abutilon mosaic virus cluster. Virus Genes 50, 63–70. https://doi.org/10.1007/s11262-014-1125-1.

Francki, R.I.B., Hatta, T., Grylls, N.E., Grivell, C.J., 1979. The particle morphology and some other properties of chloris striate mosaic virus. Ann. Appl. Biol. 91, 51–59.

Genschik, P., Criqui, M.C., Parmentier, Y., Derevier, A., Fleck, J., 1998. Cell cycle-dependent proteolysis in plants. Identification of the destruction box pathway and metaphase arrest produced by the proteasome inhibitor mg132. Plant Cell 10, 2063–2076.

Gertsman, I., Gan, L., Guttman, M., Lee, K., Speir, J.A., Duda, R.L., Hendrix, R.W., Komives, E.A., Johnson, J.E., 2009. An unexpected twist in viral capsid maturation. Nature 458, 646–650. https://doi.org/10.1038/nature07686.

Goodman, R.M., Bird, J., Thongmeearkom, P., 1977. An unusual viruslike particle associated with golden yellow mosaic of beans. Phytopathology 67, 37–42.

Gorovits, R., Fridman, L., Kolot, M., Rotem, O., Ghanim, M., Shriki, O., Czosnek, H., 2016. Tomato yellow leaf curl virus confronts host degradation by sheltering in small/midsized protein aggregates. Virus Res. 213, 304–313. https://doi.org/10.1016/j.virusres.2015.11.020.

Gorovits, R., Moshe, A., Ghanim, M., Czosnek, H., 2014. Degradation mechanisms of the Tomato yellow leaf curl virus coat protein following inoculation of tomato plants by the whitefly Bemisia tabaci. Pest Manag. Sci. 70, 1632–1639. https://doi.org/10.1002/ps.3737.

Gorovits, R., Moshe, A., Ghanim, M., Czosnek, H., 2013a. Recruitment of the host plant heat shock protein 70 by Tomato yellow leaf curl virus coat protein is required for virus infection. PLoS One 8, e70280. https://doi.org/10.1371/journal.pone.0070280.

Gorovits, R., Moshe, A., Kolot, M., Sobol, I., Czosnek, H., 2013b. Progressive aggregation of Tomato yellow leaf curl virus coat protein in systemically infected tomato plants, susceptible and resistant to the virus. Virus Res. 171, 33–43. https://doi.org/10.1016/j.virusres.2012.09.017.

Hallan, V., Gafni, Y., 2001. Tomato yellow leaf curl virus (TYLCV) capsid protein (CP) subunit interactions: implications for viral assembly. Arch. Virol. 146, 1765–1773.

Harrison, B.D., Barker, H., Bock, K.R., Guthrie, E.J., Meredith, G., Atkinson, M., 1977. Plant-viruses with circular single-stranded DNA. Nature 270, 760–762.

Hehnle, S., Wege, C., Jeske, H., 2004. The interaction of DNA with the movement proteins of geminiviruses revisited. J. Virol. 78, 7698–7706.

Héricourt, F., Blanc, S., Redeker, V., Jupin, I., 2000. Evidence for phosphorylation and ubiquitinylation of the turnip yellow mosaic virus RNA-dependent RNA polymerase domain expressed in a baculovirus-insect cell system. Biochem. J. 349, 417–425.

Hesketh, E.L., Saunders, K., Fisher, C., Potze, J., Stanley, J., Lomonossoff, G.P., Ranson, N.A., 2018. The 3.3 Å structure of a plant geminivirus using cryo-EM. Nat. Commun. 9, 2369. https://doi.org/10.1038/s41467-018-04793-6.

Hipp, K., Grimm, C., Jeske, H., Böttcher, B., 2017. Near-atomic resolution structure of a plant geminivirus determined by electron cryomicroscopy. Structure 25, 1303–1309. https://doi.org/10.1016/j.str.2017.06.013.

Hipp, K., Rau, P., Schäfer, B., Gronenborn, B., Jeske, H., 2014. The RXL motif of the African cassava mosaic virus Rep protein is necessary for rereplication of yeast DNA and viral infection in plants. Virology 462–463, 189–198. https://doi.org/10.1016/j.virol.2014.06.002.

Hipp, K., Schäfer, B., Kepp, G., Jeske, H., 2016. Properties of African cassava mosaic virus capsid protein expressed in fission yeast. Viruses 8. https://doi.org/10.3390/v8070190.

Höhnle, M., Höfer, P., Bedford, I.D., Briddon, R.W., Markham, P.G., Frischmuth, T., 2001. Exchange of three amino acids in the coat protein results in efficient whitefly transmission of a nontransmissible Abutilon mosaic virus isolate. Virology 290, 164–171.

Huang, R.K., Khayat, R., Lee, K.K., Gertsman, I., Duda, R.L., Hendrix, R.W., Johnson, J.E., 2011. The prohead-I structure of bacteriophage HK97: implications for scaffold-mediated control of particle assembly and maturation. J. Mol. Biol. 408, 541–554. https://doi.org/10.1016/j.jmb.2011.01.016.

Ingham, D.J., Pascal, E., Lazarowitz, S.G., 1995. Both bipartite geminivirus movement proteins define viral host range, but only BL1 determines viral pathogenicity. Virology 207, 191–204.

Jeske, H., 2009. Geminiviruses. In: zur Hausen, H., de Villiers, E.-M. (Eds.), Torque Teno Virus: The Still Elusive Human Pathogens, Current Topics in Microbiology and Immunology. Springer, Berlin, pp. 185–226.

Jeske, H., Menzel, D., Werz, G., 1977. Electron microscopic studies on intranuclear virus-like inclusions in mosaic-diseased Abutilon sellowianum. Reg. Phytopathol. Z. 89, 289–295.

Jupin, I., Ayach, M., Jomat, L., Fieulaine, S., Bressanelli, S., 2017. A mobile loop near the active site acts as a switch between the dual activities of a viral protease/deubiquitinase. PLoS Pathog. 13, e1006714. https://doi.org/10.1371/journal.ppat.1006714.

Kadri, A., Maiss, E., Amsharov, N., Bittner, A.M., Balci, S., Kern, K., Jeske, H., Wege, C., 2011. Engineered Tobacco mosaic virus mutants with distinct physical characteristics in planta and enhanced metallization properties. Virus Res. 157, 35–46. https://doi.org/10.1016/j.virusres.2011.01.014.

Kheyr-Pour, A., Bananej, K., Dafalla, G.A., Caciagli, P., Noris, E., Ahoonmanesh, A., Lecoq, H., Gronenborn, B., 2000. Watermelon chlorotic stunt virus from the Sudan and Iran: sequence comparison and identification of a whitefly-transmission determinant. Phytopathology 90, 629–635.

Khoo, S.K., Loll, B., Chan, W.T., Shoeman, R.L., Ngoo, L., Yeo, C.C., Meinhart, A., 2007. Molecular and structural characterization of the PezAT chromosomal toxin-antitoxin system of the human pathogen Streptococcus pneumoniae. J. Biol. Chem. 282, 19606–19618. https://doi.org/10.1074/jbc.M701703200.

Kikuno, R., Toh, H., Hayashida, H., Miyata, T., 1984. Sequence similaritiy between putative gene products of geminiviral DNAs. Nature 308, 562.

Kittelmann, K., Jeske, H., 2008. Disassembly of African cassava mosaic virus. J. Gen. Virol. 89, 2029–2036. https://doi.org/10.1099/vir.0.2008/000687-0.

Kittelmann, K., Rau, P., Gronenborn, B., Jeske, H., 2009. Plant geminivirus Rep protein induces rereplication in fission yeast. J. Virol. 83, 6769–6778.

Kleinow, T., Tanwir, F., Kocher, C., Krenz, B., Wege, C., Jeske, H., 2009. Expression dynamics and ultrastructural localization of epitope-tagged Abutilon mosaic virus nuclear shuttle and movement proteins in Nicotiana benthamiana cells. Virology 391, 212–220. https://doi.org/10.1016/j.virol.2009.06.042.

Laemmli, U.K., 1970. Cleavage of structural proteins during the assembly of the head of bacteriophage T4. Nature 227, 680–685.

Legg, J.P., Jeremiah, S.C., Obiero, H.M., Maruthi, M.N., Ndyetabula, I., Okao-Okuja, G., Bouwmeester, H., Bigirimana, S., Tata-Hangy, W., Gashaka, G., Mkamilo, G., Alicai, T., Lava Kumar, P., 2011. Comparing the regional epidemiology of the cassava mosaic and cassava brown streak virus pandemics in Africa. Virus Res. 159, 161–170. https://doi.org/10.1016/j.virusres.2011.04.018.

Liu, H., Boulton, M.I., Oparka, K.J., Davies, J.W., 2001. Interaction of the movement and coat proteins of Maize streak virus: implications for the transport of viral DNA. J. Gen. Virol. 82, 35–44. https://doi.org/10.1099/0022-1317-82-1-35.

Liu, H.T., Boulton, M.I., Davies, J.W., 1997. Maize streak virus coat protein binds single- and double-stranded DNA in vitro. J. Gen. Virol. 78, 1265–1270.

Liu, S., Briddon, R.W., Bedford, I.D., Pinner, M.S., Markham, P.G., 1999. Identification of genes directly and indirectly involved in the insect transmission of African cassava mosaic geminivirus by Bemisia tabaci. Virus Genes 18, 5–11.

Lozano-Duran, R., Bejarano, E.R., 2011. Geminivirus C2 protein might be the key player for geminiviral co- option of SCF-mediated ubiquitination. Plant Signal. Behav. 6, 999–1001.

Malik, P.S., Kumar, V., Bagewadi, B., Mukherjee, S.K., 2005. Interaction between coat protein and replication initiation protein of Mung bean yellow mosaic India virus might lead to control of viral DNA replication. Virology 337, 273–283.

Matyis, J.C., Silva, D.M., Oliveira, A.R., Costa, A.S., 1975. Purificacao e morfologia do virus do mosaico dourado do tomateiro. Summa Phytopathol. 267–273.

McDowell, G.S., Philpott, A., 2013. Non-canonical ubiquitylation: mechanisms and consequences. Int. J. Biochem. Cell Biol. 45, 1833–1842. https://doi.org/10.1016/j.biocel.2013.05.026.

Mou, F., Wills, E., Baines, J.D., 2009. Phosphorylation of the U(L)31 protein of herpes simplex virus 1 by the U(S)3-encoded kinase regulates localization of the nuclear

envelopment complex and egress of nucleocapsids. J. Virol. 83, 5181–5191. https://doi.org/10.1128/JVI.00090-09.
Noris, E., Vaira, A.M., Caciagli, P., Masenga, V., Gronenborn, B., Accotto, G.P., 1998. Amino acids in the capsid protein of tomato yellow leaf curl virus that are crucial for systemic infection, particle formation, and insect transmission. J. Virol. 72, 10050–10057.
Novikova, O., Topilina, N., Belfort, M., 2014. Enigmatic distribution, evolution, and function of inteins. J. Biol. Chem. 289, 14490–14497. https://doi.org/10.1074/jbc.R114.548255.
Palanichelvam, K., Kunik, T., Citovsky, V., Gafni, Y., 1998. The capsid protein of tomato yellow leaf curl virus binds cooperatively to single-stranded DNA. J. Gen. Virol. 79, 2829–2833.
Patil, B.L., Fauquet, C.M., 2009. Cassava mosaic geminiviruses: actual knowledge and perspectives. Mol. Plant Pathol. 10, 685–701. https://doi.org/10.1111/j.1364-3703.2009.00559.x.
Priyadarshini, P.C.G., Savithri, H.S., 2009. Kinetics of interaction of Cotton leaf curl Kokhran virus-Dabawali (CLCuKV-Dab) coat protein and its mutants with ssDNA. Virology 386, 427–437. https://doi.org/10.1016/j.virol.2009.01.016.
Romero-Barrios, N., Vert, G., 2018. Proteasome-independent functions of lysine-63 polyubiquitination in plants. New Phytol. 217, 995–1011. https://doi.org/10.1111/nph.14915.
Rossmann, M.G., 2013. Structure of viruses: a short history. Q. Rev. Biophys. 46, 133–180. https://doi.org/10.1017/S0033583513000012.
Ryan, C.A., Annunziato, A.T., 2001. Separation of histone variants and post-translationally modified isoforms by triton/acetic acid/urea polyacrylamide gel electrophoresis. Curr. Protoc. Mol. Biol. Ed. Frederick M Ausubel Al Chapter 21, Unit 21.2. ⟨https://doi.org/10.1002/0471142727.mb2102s45⟩.
Rybicki, E.P., 2015. A top ten list for economically important plant viruses. Arch. Virol. 160, 17–20. https://doi.org/10.1007/s00705-014-2295-9.
Sahtoe, D.D., Sixma, T.K., 2015. Layers of DUB regulation. Trends Biochem. Sci. 40, 456–467. https://doi.org/10.1016/j.tibs.2015.05.002.
Sato, T., Sako, K., Yamaguchi, J., 2014. Assay for proteasome-dependent protein degradation and ubiquitinated proteins. In: Jorrin-Novo, J.V., Komatsu, S., Weckwerth, W., Wienkoop, S. (Eds.), Plant Proteomics: Methods and Protocols. Humana Press, Totowa, NJ, pp. 655–663.
Schmidt, T., Striebinger, H., Haas, J., Bailer, S.M., 2010. The heterogeneous nuclear ribonucleoprotein K is important for Herpes simplex virus-1 propagation. FEBS Lett. 584, 4361–4365. https://doi.org/10.1016/j.febslet.2010.09.038.
Shechter, D., Dormann, H.L., Allis, C.D., Hake, S.B., 2007. Extraction, purification and analysis of histones. Nat. Protoc. 2, 1445–1457. https://doi.org/10.1038/nprot.2007.202.
Shen, W., Bobay, B.G., Greeley, L.A., Reyes, M.I., Rajabu, C.A., Blackburn, R.K., Dallas, M.B., Goshe, M.B., Ascencio-Ibáñez, J.T., Hanley-Bowdoin, L., 2018. Sucrose non-fermenting 1-related protein kinase 1 phosphorylates a geminivirus Rep protein to impair viral replication and infection. Plant Physiol. 178, 372–389. https://doi.org/10.1104/pp.18.00268.
Stes, E., Laga, M., Walton, A., Samyn, N., Timmerman, E., De Smet, I., Goormachtig, S., Gevaert, K., 2014. A COFRADIC protocol to study protein ubiquitination. J. Proteome Res. 13, 3107–3113. https://doi.org/10.1021/pr4012443.
Unseld, S., Frischmuth, T., Jeske, H., 2004. Short deletions in nuclear targeting sequences of African cassava mosaic virus coat protein prevent geminivirus twinned particle formation. Virology 318, 89–100.
Unseld, S., Höhnle, M., Ringel, M., Frischmuth, T., 2001. Subcellular targeting of the coat protein of African cassava mosaic geminivirus. Virology 286, 373–383.
Von Arnim, A., Frischmuth, T., Stanley, J., 1993. Detection and possible functions of African cassava mosaic virus DNA B gene products. Virology 192, 264–272. https://doi.org/10.1006/viro.1993.1029.
Walton, A., Stes, E., Cybulski, N., Van Bel, M., Iñigo, S., Durand, A.N., Timmerman, E., Heyman, J., Pauwels, L., De Veylder, L., Goossens, A., De Smet, I., Coppens, F., Goormachtig, S., Gevaert, K., 2016. It's time for some “site”-seeing: novel tools to monitor the ubiquitin landscape in Arabidopsis thaliana. Plant Cell 28, 6–16. https://doi.org/10.1105/tpc.15.00878.
Wege, C., Jeske, H., 1998. Abutilon mosaic geminivirus proteins expressed and phosphorylated in Escherichia coli. J. Phytopathol. 146, 613–621.
Wisner, T.W., Wright, C.C., Kato, A., Kawaguchi, Y., Mou, F., Baines, J.D., Roller, R.J., Johnson, D.C., 2009. Herpesvirus gB-induced fusion between the virion envelope and outer nuclear membrane during virus egress is regulated by the viral US3 kinase. J. Virol. 83, 3115–3126. https://doi.org/10.1128/JVI.01462-08.
Wulfmeyer, T., Polzer, C., Hiepler, G., Hamacher, K., Shoeman, R., Dunigan, D.D., Van Etten, J.L., Lolicato, M., Moroni, A., Thiel, G., Meckel, T., 2012. Structural organization of DNA in chlorella viruses. PLoS One 7, e30133. https://doi.org/10.1371/journal.pone.0030133.
Yaakov, N., Levy, Y., Belausov, E., Gaba, V., Lapidot, M., Gafni, Y., 2011. Effect of a single amino acid substitution in the NLS domain of Tomato yellow leaf curl virus-Israel (TYLCV-IL) capsid protein (CP) on its activity and on the virus life cycle. Virus Res. 158, 8–11. https://doi.org/10.1016/j.virusres.2011.02.016.
Zerbini, F.M., Briddon, R.W., Idris, A., Martin, D.P., Moriones, E., Navas-Castillo, J., Rivera-Bustamante, R., Roumagnac, P., Varsani, A., ICTV Report Consortium, 2017. ICTV virus taxonomy profile: geminiviridae. J. Gen. Virol. 98, 131–133. https://doi.org/10.1099/jgv.0.000738.
Zhang, W., Olson, N.H., Baker, T.S., Faulkner, L., Agbandje-McKenna, M., Boulton, M., Davies, J.W., McKenna, R., 2001. Structure of the Maize streak virus geminate particle. Virology 279, 471–477.